12 Kitaev Magnets

Simon Trebst
Institute für Theoretische Physik, Universität zu Köln
Zülpicher Straße 77, 50937 Köln

Contents

1 Introduction **2**

2 Spin liquids **2**
2.1 Frustrated magnets 3
2.2 Classical spin liquids 5
2.3 Quantum spin liquids 7

3 Kitaev honeycomb model **8**
3.1 Fractionalization and spin liquid ground states 9
3.2 Thermal signatures of fractionalization 10

4 Spin-orbit entangled Mott insulators **12**

5 Kitaev materials **15**
5.1 Honeycomb iridates Na_2IrO_3 and Li_2IrO_3 16
5.2 α-$RuCl_3$ 18
5.3 Other materials 19

6 Outlook **20**

E. Pavarini and E. Koch (eds.)
Orbital Physics in Correlated Matter
Modeling and Simulation Vol. 13
Forschungszentrum Jülich, 2023, ISBN 978-3-95806-689-2
http://www.cond-mat.de/events/correl23

1 Introduction

Kitaev materials – spin-orbit entangled Mott insulators with strong bond-directional Ising-like interactions – have attracted considerable interest over the past 15 years as candidate compounds to realize quantum spin liquid physics in experiment. This chapter will guide you on a journey through this field, which many expect to be fertile ground for many future discoveries, both experimentally and theoretically. We will start from building a conceptual perspective on the broader context by first providing a gentle introduction to spin liquids in frustrated magnets, both in the classical and quantum realm. A key player in this field is the Kitaev honeycomb model, to which we will devote a separate section. We will then move the conceptual underpinning to the materials side and introduce the broad class of spin-orbit entangled Mott insulators that are found in $4d$ and $5d$ materials and see how they distinguish themselves from more conventional Mott insulators, which have long been discussed in the context of cuprates and other $3d$ materials. Having set the stage as such, we will then turn to the family of Kitaev materials and discuss some prominent members such as $RuCl_3$ and the iridates Na_2IrO_3 and Li_2IrO_3. The chapter will close with an overview of more recent advances and an outlook what to expect in the near future.

This chapter is based on lecture notes [1], which I have prepared for a 2017 Jülich spring school under the heading "Topological Matter – Topological Insulators, Skyrmions and Majoranas" (48th IFF Spring School). Together with Ciarán Hickey these lecture notes were later turned into a substantially expanded 2022 review article [2] that gives a more in-depth introduction to this field. We should mention that a few other closely related reviews might be good pointers for the interested reader, such as two early reviews on spin-orbit entangled materials [3, 4], along with review-style articles directed towards Kitaev materials [5, 6]. We will mention additional, topical reviews in the subsequent sections that guide to pedagogical introductions or in-depth discussions of the broader context of Kitaev materials.

2 Spin liquids

Let us start our exploration of the conceptual background of (quantum) magnets by reminding ourselves of a paradigm that was first established in the context of the Ising model – spontaneous symmetry breaking. Cast in most general terms, the idea here is that the low-temperature ground state of a system has *less symmetry* than the high-temperature phase which still reflects all symmetries of the underlying Hamiltonian. Case in point of the Ising model is the magnetic ordering of the ground state which breaks the Z_2 symmetry of the original Ising Hamiltonian. This happens at a finite-temperature phase transition, at which it is precisely this Z_2 symmetry, still present in the high-temperature paramagnetic phase, which is spontaneously broken as one traverses the transition towards the low-temperature magnetically ordered phase. This is all very well understood – the finite-temperature transition itself arises from the competition of energy and entropy, while the formation of magnetic order accompanying the spontaneous symmetry breaking can be elegantly captured in terms of Landau-Ginzburg-Wilson theory.

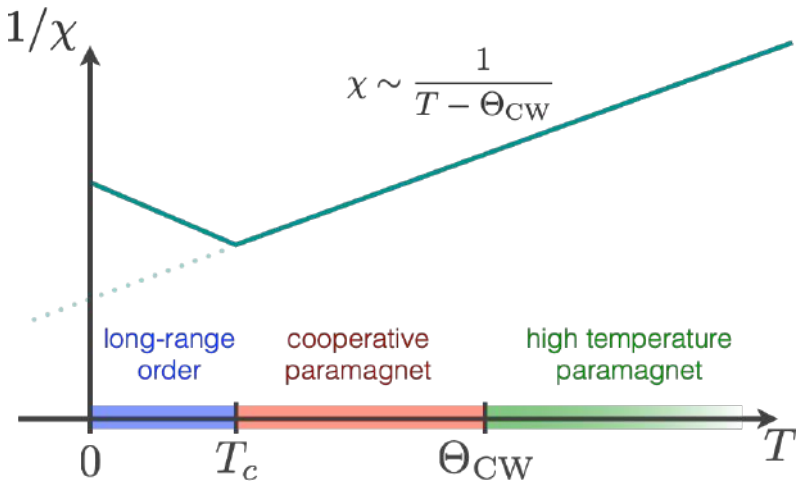

Fig. 1: Frustrated magnetism. *While conventional magnets are expected to show a magnetic ordering transition around the temperature scale associated with the Curie-Weiss scale $\Theta_{\rm CW}$, frustrated magnets instead exhibit an expanded temperature regime (below $\Theta_{\rm CW}$) in which the magnetic susceptibility χ continues to follow a Curie-Weiss law – as if it were still a paramagnet. This regime is often referred to as "cooperative paramagnet". Eventually, the system might order at some very low temperature scale T_c.*

But, quite intriguingly, the exact opposite can also happen – a magnetic system's ground state(s) can have *more symmetry* than the original Hamiltonian and associated high-temperature phase. This is, in fact, what one might define as one of the trademarks of frustrated magnets and the *emergence* of spin liquid physics.

2.1 Frustrated magnets

A frustrated magnet distinguishes itself from a conventional magnet by the absence or strong suppression of the finite-temperature phase transition to a magnetically ordered state. For any conventional magnet, we expect that this phase transition occurs roughly at the Curie-Weiss temperature $\Theta_{\rm CW}$ (set by the various magnetic couplings of a given system). For a frustrated magnet, in contrast, the magnetic susceptibility χ continues to follow a Curie-Weiss law, i.e.

$$\chi \propto \frac{1}{T - \Theta_{\rm CW}} ,$$

even way below the Curie-Weiss temperature. That is, the system keeps behaving as if it were in a paramagnetic phase. But since the system keeps loosing entropy as one goes to lower and lower temperature, there must be a distinction from the high-temperature paramagnet after all. In fact, the system might build up *local* correlations, which however do not reach correlation lengths of the order of the system size and the system therefore eludes the formation of long-range magnetic order. One often refers to this regime as "cooperative paramagnet" – a precursor of the spin liquid physics we might see at the very lowest temperatures (and which we will discuss in the next section) if that physics is not preempted by a magnetic ordering transition. The latter might occur also in a frustrated magnet, albeit at a much lower temperature than in a

conventional magnet as depicted in Fig. 1. In fact, the ratio of the Curie-Weiss temperature and the suppressed transition temperature T_c

$$f = \frac{\Theta_{\rm CW}}{T_c}$$

is a good quantifier of how frustrated a certain system really is and to distinguish a conventional magnet from a "highly-frustrated" magnet. For a conventional magnet $f \approx 1$, while one speaks of a highly-frustrated magnet if $f \gtrsim 10$. In the most extreme case of a system that exhibits no magnetic order transition whatsoever f goes to infinity.

So you might ask what is the microscopic origin of such frustration effects and the ultimate suppression of any magnetic order? The source here are *competing interactions* that cannot be simultaneously satisfied, e.g., by a single state (such as a magnetically ordered one). Instead it is a multitude of states that are all found to be equally well suited to satisfy most of the interactions, that is one finds a manifold of states that all exhibit the same (minimal) energy, though they might differ in their microscopic details. Such an emergence of a low-temperature *residual entropy* really is the defining signature of a frustrated magnet.

One of the most cited and earliest examples here is the triangular lattice Ising antiferromagnet, depicted on the left in Fig. 2. If all couplings are antiferromagnetic, each triangle will exhibit one bond that is left unsatisfied by the choice of the spin alignment around it. Going to a finite lattice with many such triangles this will lead to a ground-state degeneracy that will grow extensively with the number of spins (triangles). This emergence of a residual entropy was first discovered and quantitatively described by Wannier in a seminal 1950 work [7, 8]. Today, we refer to the underlying mechanism as *geometric frustration* to indicate that the source of residual entropy formation really arises from the underlying (non-bipartite) lattice geometry, which is simply non-commensurable with the formation of an antiferromagnetic Néel state.[1] Famous other examples of such non-bipartite lattice geometries are the kagome lattice in two spatial dimensions and the pyrochlore lattice in three spatial dimensions.

Another source of frustration, which will be more relevant in the context of the current chapter, is so-called *exchange frustration*. Consider the arrangement on the right-hand side of Figure 2 where a classical, three component Heisenberg spin is subject to three competing interactions that want to align this spin along one of the three principal spin axes via a pairwise interaction

$$\text{blue bond:} \quad S_i^x S_j^x \qquad \text{green bond:} \quad S_i^y S_j^y \qquad \text{brown bond:} \quad S_i^z S_j^z$$

to match a correspondingly $\{x, y, z\}$-aligned spin on the other side of the bond. Due to the orthogonality of the three principal spin axes, it is impossible to simultaneously satisfy all three exchange terms. Instead, if one picks one of the three principal spin axes (which energetically is more favorable than pointing, e.g., along the [111] direction) one has three equally good (or bad) choices, which again points to the formation of a residual entropy if one continues the

[1] One has to be rather careful, though, in designating geometric frustration to certain spin model. Note, for instance, that the antiferromagnetic *Heisenberg* model on the triangular lattice is *not* subject to geometric frustration. Here the spins will, at low temperatures, simply align in one of two 120 degree ordered states and as such there is no residual entropy.

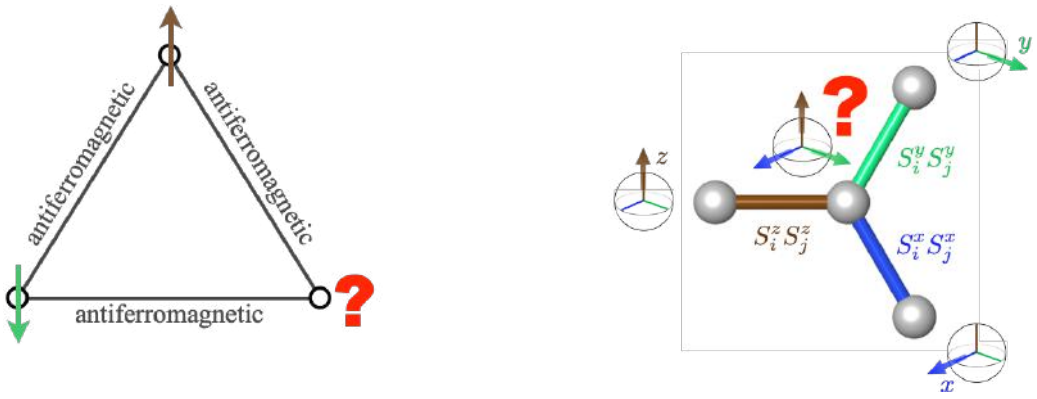

Fig. 2: Sources of Frustration. *(left) Geometric frustration arises from non-bipartite lattice geometries which are incompatible with the formation of a Néel state in antiferromagnetic systems, such as an Ising antiferromagnet on the triangular lattice. (right) Exchange frustration arises from competing interactions that cannot be simultaneously satisfied, even for a single site. An example of this are the three bond-directional interactions favoring alignment of the spins in orthogonal directions.*

tricolored bond assignment for all bonds of, say, a honeycomb lattice. Such exchange frustration is equally capable of suppressing magnetic order as the geometric frustration introduced above. Notably, exchange frustration can also occur for *ferro*magnetic interactions on a bipartite lattice geometry (as in the example above) – that is, in systems, which typically are considered to give rise to simple ferromagnets.

2.2 Classical spin liquids

We now want to consider a frustrated magnet, which indeed shows no magnetic order down to zero temperature. Examples in the realm of classical spins are the triangular lattice Ising antiferromagnet – the principal example of geometric frustration in Figure 2, and the Heisenberg model with bond-directional (ferromagnetic) Ising-like interactions on the honeycomb lattice – the principal example of exchange frustration in Figure 2. The latter example, which in fact is the Kitaev model of the subsequent section, will stay with us throughout the chapter, but for now we might think of it as simply a classical, spin-anisotropic Heisenberg model with no magnetic ordering. For both systems we know that as a result of frustration there will be no single, magnetically ordered ground state but instead there will be a significant residual entropy at zero temperature – in these cases extensive manifolds of states that all equally well satisfy the energetics of the underlying Hamiltonians. But what is the difference between these state manifolds and the high-temperature paramagnet? And can we identify, as alluded to in the introduction of this section, a higher symmetry in these ground states than what the Hamiltonians suggest?
The answers to these questions will introduce us to the concept of *classical spin liquids*. Let us approach such a classical spin liquid by considering the ground state manifold of the bond-directional Heisenberg model on the honeycomb lattice, i.e. the classical Kitaev model with ferromagnetic interactions. The aforementioned exchange frustration in this model results in

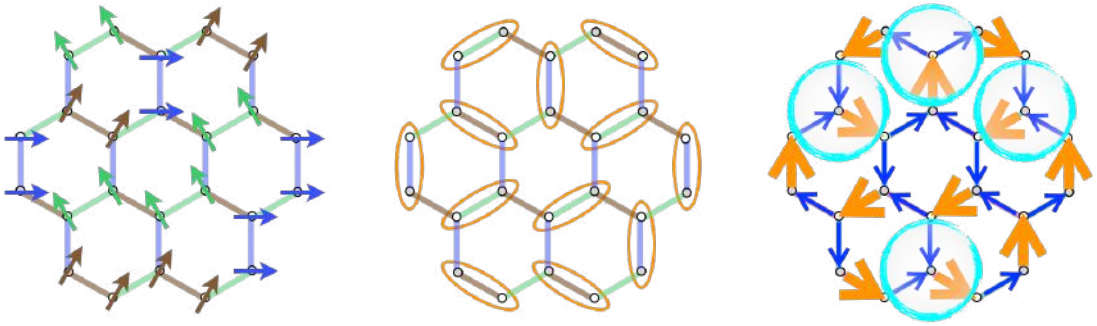

Fig. 3: Coulomb phase. *(left) Ground-state configuration of the classical Kitaev model where the bond-directional Ising-like interactions pair up spins in "dimers" (middle) Dimer covering of the honeycomb lattice, corresponding to the spin configuration on the left. (right) Mapping to a divergence-free magnetic field configuration where each site has an equal number of incoming and outgoing field lines if the orange arrows carry twice the field strengths of the blue arrows.*

a large number of ground states, which can be characterized as illustrated in the left panel of Figure 3: every spin pairs up with one of its three neighboring spins to form a "dimer" of spins pointing along one of the three principal spin axes (such that exactly one of three interaction terms per spin is fully satisfied while two remain completely unsatisfied). In more abstract terms, any such spin configuration can be conceptualized as a dimer covering of the honeycomb lattice[2] as illustrated in the middle panel of Fig. 3 for the exact same spin configuration. This simplifies the description, as a whole lot is known about dimer coverings such as, for instance, how many there are for a given lattice geometry and system size – that is, a direct measure of the residual entropy of our spin model at hand. Even more enticing is the fact that we can rewrite the local condition of "every spin is part of exactly one dimer" into a configuration of an artificial magnetic field that is divergence-free at every site, see the right panel in Fig. 3. This is a powerful correspondence, which tells us that the ground state of the classical Kitaev model (or the triangular lattice Ising antiferromagnet) is described by a *Coulomb phase* [9]. It readily lets us conclude that there are longer range, power-law decaying correlations in these ground states and that the elementary excitations are violations of the divergence-free conditions – magnetic monopoles. In other words, the ground state manifold of our classical magnets are described by *emergent magnetostatics*, a much more elegant description than what we might have anticipated when considering the quite ordinary nature of their underlying Hamiltonians.

It is precisely this theme of an *emergent* description of the low-energy states that sets apart the low-temperature phase of a highly frustrated magnet from both the high-temperature paramagnetic phase, which does not allow for an equally elegant description, or the symmetry-broken ground state of a conventional magnet. This naturally brings us to the question what additional effects zero-temperature quantum fluctuations might entail. On a pessimistic note one might argue that they will simply split the accidental degeneracy of the aforementioned classical ground

[2]Notably, Wannier showed that every ground state configuration of the triangular lattice Ising antiferromagnet can also be mapped to a dimer covering of the honeycomb lattice by marking the unsatisfied bonds of the triangular lattice to its dual honeycomb lattice. As such, all arguments applied to the ground state manifold of the classical Kitaev model also apply to the Ising case.

states in a mechanism referred to as order-by-disorder and thereby destroy all beauty. But this is, fortunately, not true after all and there will be even more to discover when going deep into the quantum realm of strongly fluctuating magnetic moments.

2.3 Quantum spin liquids

Like their classical counterparts, quantum spin liquids are not defined by the absence of magnetic order, but instead by the emergence of additional structures. As one might expect for a proper quantum system, this additional structure comes in the form of entanglement, or more precisely, *long-range entanglement* of the underlying quantum mechanical degrees of freedom. To discuss this, we need to recall some basic notions of quantum many-body entanglement. The latter is often quantified by an entanglement entropy defined via the reduced density matrix for a bipartition of the system into two subsystems (say, A and B). This entanglement entropy is quite distinct from a conventional thermal entropy (familiar from any statistical mechanics course) in that it is not extensive, but instead obeys a boundary law, i.e., it scales with the length of the boundary ∂A separating the two subsystems

$$S = a \cdot \partial A - \gamma + \dots ,$$

where a is some non-universal prefactor in the boundary law, γ refers to an important $O(1)$ correction, and the dots indicate further subleading terms. Our focus here should, in fact, be on the $O(1)$ correction γ that indicates an emergent topological quantum field theory (TQFT) description of the quantum state at hand – that is, an emergent structure that was not present in the Hamiltonian giving rise to the ground state in front of us, somewhat akin to what we had encountered in the classical context but on a whole new level. A TQFT is a complex theory whose constituents are, in general, different types of anyonic particles. An elementary example is the Ising TQFT with its ground state, denoted as 1, and two additional σ and ψ particles which have quantum dimensions[3] $1, \sqrt{2}, 1$, respectively. What is relevant here is that these quantum dimensions define the topological correction of the entanglement entropy [10, 11] in a universal manner as

$$\gamma = \ln \left(\sqrt{\sum d_i^2} \right) ,$$

which in the case of the Ising TQFT reveals a correction of $\gamma = \ln 2$. Importantly, the topological correction to the boundary law always results in a negative correction to the leading boundary-law. This is important as it indicates that we cannot deform the ground-state wavefunction into a simple product state, in which the boundary-law contribution would vanish and thereby turn the entanglement entropy negative – a scenario that is as forbidden as a negative thermal entropy. As such the emergence of such a topological correction instead signals the formation of long-range entanglement that can only be destroyed by driving the system through a quantum phase transition.

[3] The quantum dimension is a measure of how fast a Hilbert space spanned by N such particles grows with the number N. For conventional quantum spin-1/2 we are used to the idea that their quantum dimension is 2, while for the σ particle in the Ising TQFT it is apparently $\sqrt{2}$.

If the ground state of a quantum spin model exhibits such a form of long-range entanglement we have discovered a topological quantum spin liquid – a spin analogue of a fractional quantum Hall state as first envisioned by Kalmeyer and Laughlin [12] back in 1987. We will shortly see such a topological quantum spin liquid as the ground state of the Kitaev model in a magnetic field, and its relevance in the context of half-integer thermal quantum Hall states in the discussion of $RuCl_3$ in the last section.

The above description of quantum spin liquids is a pretty high-brow introduction using the abstract measures of entanglement, which theorists might love as a distinct measure but experimentalists will have a hard time to measure in the foreseeable future. Let us therefore introduce an alternate approach to describe the emergent phenomena of a quantum spin liquid, which might also be closer to experimental reality.

This alternative description of a spin liquid uses the concepts of *fractionalization* and *emergent gauge theories* – concepts that will come to life in the next section when we discuss the exact analytical solution of the quantum Kitaev model. Here we will simply introduce the main ideas and point the interested readers to the excellent review by Lucile Savary and Leon Balents on the subject [13]. In this framework, quantum spin liquids are emergent descriptions of the ground states of quantum magnets in which the elementary degrees of freedom, typically magnetic moments with spin-1/2 or spin-1, decompose into novel, fractionalized quantum particles – a parton (such as a Majorana or complex fermion) coupled to a gauge field. One then distinguishes the different types of possible quantum spin liquids by their different gauge structure into (i) Z_2 quantum spin liquids, (ii) $U(1)$ quantum spin liquids, and (iii) chiral spin liquids (with an emergent Chern-Simons theory). The aforementioned topological quantum spin liquid is an example of the latter, while the Kitaev model (without a magnetic field) is often considered as the quintessential model harboring a Z_2 quantum spin liquid ground state.

3 Kitaev honeycomb model

Let us now turn to the main motivation that has set off the search for Kitaev materials – the original Kitaev honeycomb model [14] and its rich physics [15]. The model itself is a variant of a quantum compass model [16], as discussed in much broader context in the accompanying chapter of Jeroen van den Brink. As such it has a deceivingly simple looking Hamiltonian of bond-directional, Ising-like interactions that couple elementary quantum spin-1/2 degrees of freedom on a honeycomb lattice

$$H_{\text{Kitaev}} = \sum_{i,\gamma} K_\gamma \, S_i^\gamma S_j^\gamma \, ,$$

where $\gamma = x, y, z$ denotes the three principal directions of the honeycomb lattice (depicted in blue/green/brown in Figure 4) and, at the same time, the three principal spin orientations.

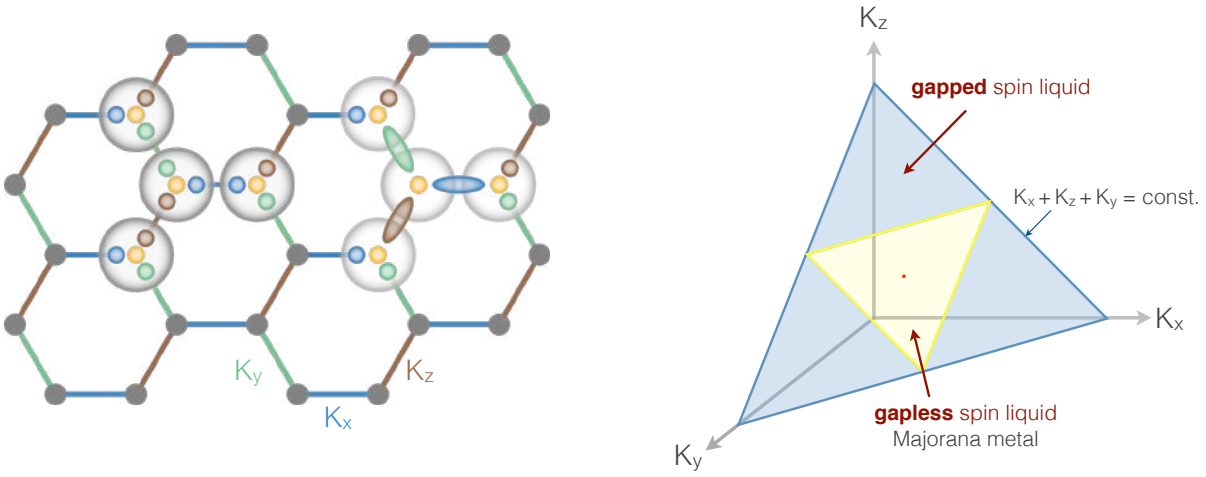

Fig. 4: Kitaev model. *(left) Bond-directional Ising-like interactions between spin-1/2 moments make the Kitaev model an example of a quantum compass model. Its analytical solution is sketched as the decomposition of the original spin degrees of freedom into four Majorana fermions (circles), which are then recombined in a pairwise fashion to result in a Z_2 gauge field on the bonds (ellipses) and a free, itinerant Majorana fermion (yellow circle) hopping on the lattice in the background of a static Z_2 gauge field. (right) The phase diagram of the Kitaev model in the plane $K_x+K_y+K_z = 1$, which exhibits three gapped spin liquid phases and an extended gapless spin liquid phase around the point of isotropic coupling.*

3.1 Fractionalization and spin liquid ground states

What sets this spin model apart from basically every other interacting quantum spin system is that Alexei Kitaev could solve this model exactly at zero temperature, i.e., he could analytically derive its entire ground-state phase diagram [14]. The latter is depicted in the right panel of Figure 4 and shows four highly non-trivial ground states as a function of the coupling parameters K_x, K_y, and K_z plotted in the plane defined by $K_x+K_y+K_z = 1$. If one of the three couplings dominates, corresponding to the light blue triangles, one finds a topological spin liquid ground state, i.e., a gapped spin liquid that is characterized by a non-trivial $\gamma = \ln 2$ correction to the boundary-law entanglement scaling and which corresponds to a toric code [17] phase. The phase around the point of isotropic coupling $K_x = K_y = K_z$ is, in contrast, a gapless spin liquid. The nature of this gapless phase becomes apparent when briefly describing how Kitaev solved the underlying spin model.

The analytical approach is quite ingenious in that it directly employs the fractionalization of the elementary spin degrees of freedom. Every spin-1/2 is rewritten in terms of four Majorana fermions (as depicted schematically by the four circles on the left in Figure 4), which are subsequently recombined by fusing two such Majorana fermions adjacent to a given bond into a single Z_2 variable on every bond (depicted by the ellipses in Figure 4). The latter is the Z_2 gauge field, while the "left-over" fourth Majorana fermion per spin is the complementary parton degree of freedom. Kitaev's solution thus explicitly introduces the emergent fractionalized degrees of freedom via an exact operator decomposition. Importantly, these two degrees

of freedom have very different dynamics. While the Majorana fermion is free to traverse the lattice (as a free fermion), the Z_2 gauge field turns out to be completely static, i.e., it does not fluctuate and any gauge excitations (so-called visons) are static as well and cannot move at all. This makes the emergent lattice gauge theory description of the Kitaev model particularly simple[4] and amenable to an exact solution. The problem factorizes, in that one can first identify the ground state of the gauge field – which due to another ingenious contribution of Elliott Lieb [18] we can readily identify with the flux-free configuration – and then solve for the free Majorana fermion problem with this fixed gauge configuration. But the latter is also trivial, since we know very well what the spectrum of free fermions on a honeycomb lattice is from the study of non-interacting electrons in graphene – a band structure with a Dirac cone dispersion, where due to the particle-hole symmetry of Majorana fermions the ground state of the spin model sits exactly at the tip of this Dirac cone. Returning to the phase diagram of the Kitaev model, this picture of Majorana fermions hopping in the background of a Z_2 lattice gauge structure, lets us readily understand the gapless quantum spin liquid in the center of the phase diagram as a Majorana metal (or, more precisely, a semi-metal with a point-singular Fermi surface due to the Dirac cone in the Majorana band structure).

Going away from the pure Kitaev model, its analytical solution still allows to understand the effect of certain perturbations. For instance, if one applies a magnetic field in the (111)-direction, i.e., a field that couples to all three spin components, one introduces a mass term in the Dirac equation. As a consequence the gapless spin liquid gaps out and turns into a chiral spin liquid (with non-Abelian topological order and gapless edge modes). When rephrased in terms of *complex* fermions this gapped state corresponds to a p-wave superconductor [19], which one can conceptualize to undergo a Higgs transition to a gapless metal that, recast into the language of the quantum spin model, would correspond to a gapless $U(1)$ spin liquid (with a spinon Fermi surface). It has been argued that this indeed what happens for the *anti*ferromagnetic Kitaev model for an intermediate-strength magnetic field [20–23]. Another important perturbation of the pure Kitaev model is the inclusion of an isotropic Heisenberg interaction [24, 25], which endows the vison excitations of the Z_2 gauge field with their own dynamics [26], i.e., they can start to disperse, become soft, condense and thereby drive the system into a magnetically ordered state. Of course, one could consider many other perturbations to the Kitaev model – a topos which we will return to when discussing the miscroscopics of the actual materials considered to realize some of this Kitaev physics.

3.2 Thermal signatures of fractionalization

Staying on the conceptual level, let us instead turn to the finite-temperature characteristics of the Kitaev model. While such features are not amenable to a direct analytical treatment, they can be captured by numerically exact quantum Monte Carlo (QMC) simulations. At first sight, this might sound counter-intuitive as the spin Hamiltonian seems to exhibit a strong sign prob-

[4] Typically one would expect to find a *fluctuating* gauge field, which then would have required further steps such as a mean-field decoupling, i.e., the application of some approximative approach.

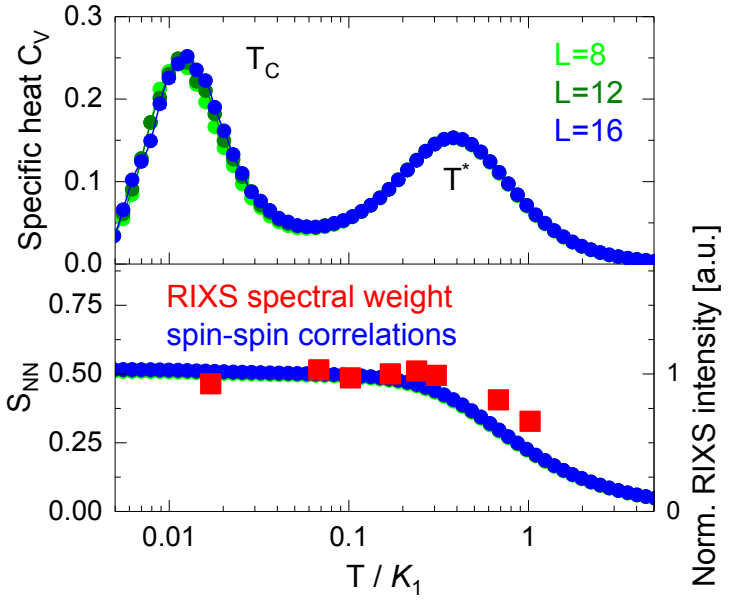

Fig. 5: Thermal signatures of fractionalization. *(top) The specific heat exhibits a characteristic two-peak structure. The feature at the higher temperature scale T^* is a thermal crossover associated with the fractionalization of the elementary spin degrees of freedom, while the lower temperature scale T_c is associated with the onset of order in the Z_2 gauge sector (for finite system sizes). (bottom) The nearest-neighbor spin-spin correlations are found to saturate already at T^*, the higher temperature scale. This is in very good agreement with resonant inelastic X-ray spectroscopy (RIXS) measurements discussed in Section 5. Figure reproduced from Ref. [27].*

lem [28] – at least when looking at it from the perspective of traditional QMC techniques such as the stochastic series expansion (SSE) [29], which is typically the first choice of QMC for quantum spin models. But at second sight and inspired by the exact solution, one should instead set up a QMC approach that samples in the fractionalized basis of Majorana fermions and the Z_2 gauge field. That is, an approach that samples the many different Z_2 gauge field configurations which become relevant at finite temperature as one allows for the thermal excitation of visons, while solving for the respective free Majorana fermion models for such modified Z_2 gauge configurations. This is precisely what Yuki Motome's group has spearheaded to arrive at a quasi-exact solution of the finite-temperature physics of the Kitaev model [30].

The key features of the thermodynamic behavior of the Kitaev model are summarized in Figure 5. The specific heat shows a distinct two-peak structure that is intimately linked to the physics of the Kitaev model. The higher-temperature feature appears at the scale of the exchange couplings and indicates the fractionalization of the elementary spin degrees of freedom and the formation of a Majorana fermion band structure. This fractionalization is a purely *local* phenomenon and as such the higher-peak is in fact a crossover phenomenon (as opposed to a phase transition, which due to its diverging length scales is rather sensitive to finite system sizes and therefore exhibits strong finite-size scaling effects whereas a crossover peak is completely insensitive to system sizes as found here). The second, lower-temperature feature is hugely

suppressed and occurs at a temperature scale of order $T_c \approx K/100$, i.e., two orders of magnitude lower than the high-temperature feature (note the logarithmic scale of the horizontal axis in Figure 5). This second feature is found to be associated with the ordering of the Z_2 gauge field, i.e., it is at this temperature scale that the system enters the flux-free ground state of the Z_2 lattice gauge theory. Above this temperature scale one finds thermally excited vison excitations and as such one might not be surprised to hear that the magnitude of this temperature scale is linked to the size of the vison gap [31]. Now, in two spatial dimensions (as it is the case for a honeycomb lattice geometry) such a vison excitation is a *point-like* excitation, e.g., a Z_2 flux threaded through a single plaquette, which can easily proliferate. This is an important observation which points us to the fact that in the thermodynamic limit of very large system sizes, this lower-temperature ordering transition scales to zero temperature, i.e., ceases to exist. This is a well known statement about two-dimensional Z_2 lattice gauge theories [32, 33], which in the context of the Kitaev model, tells us that the zero-temperature quantum spin liquids of the ground-state phase diagram are all unstable to finite-temperature fluctuations.[5] This puts the higher-temperature crossover feature back into the focus of a potential experimental signature of Kitaev materials. Indeed it should be noted that this crossover goes hand-in-hand with a build-up of nearest-neighbor spin-spin correlations as shown in the lower panel of Figure 5. Such strong correlations between neighboring spins (but not beyond) are indeed another hallmark of the Kitaev spin liquid states [35], which is also reflected in their dynamical structure factor [36, 37] and response in resonant inelastic X-ray spectroscopy (RIXS) [38, 27].

4 Spin-orbit entangled Mott insulators

Let us now enter the realm of materials physics and ask where we might look for microscopic situations that enable the emergence of Kitaev physics. At this stage, probably the most distinct feature of the Kitaev Hamiltonian is its lack of an $SU(2)$ spin symmetry and the bond-directionality of its interactions – both of which features that do not come naturally in conventional electronic Mott insulators, which typically exhibit spin-isotropic Heisenberg interactions and bond-by-bond variations are often limited to differences of the respective coupling strengths. So, we need to look further and this is where models of orbital moments might come to mind – for these it is quite natural to expect a strong bond-directionality and anisotropic interactions. Think, for instance, of a p-orbital model with p_x, p_y, and p_z orbital degrees of freedom where, simply due to the different spatial shapes and alignments of these three orbitals, the interactions in x, y, and z direction will take an Ising-like form, i.e., p_x orbitals couple strongly with one another along the x-direction but not at all along the y or z-directions and similarly for the other orbital components. So orbital physics seems to be the right ingredient to realize Kitaev-like interactions, but then orbital-only models are rare to find.

[5] As a side remark we note that this situation is very different for Kitaev models in three spatial dimensions [34], where the elementary vison excitations are extended flux loops and thereby allow for a different competition between energy and entropy leading to the existence of a true finite-temperature gauge ordering transitions, albeit ones that are still suppressed by two orders of magnitude with regard to the coupling strength [31].

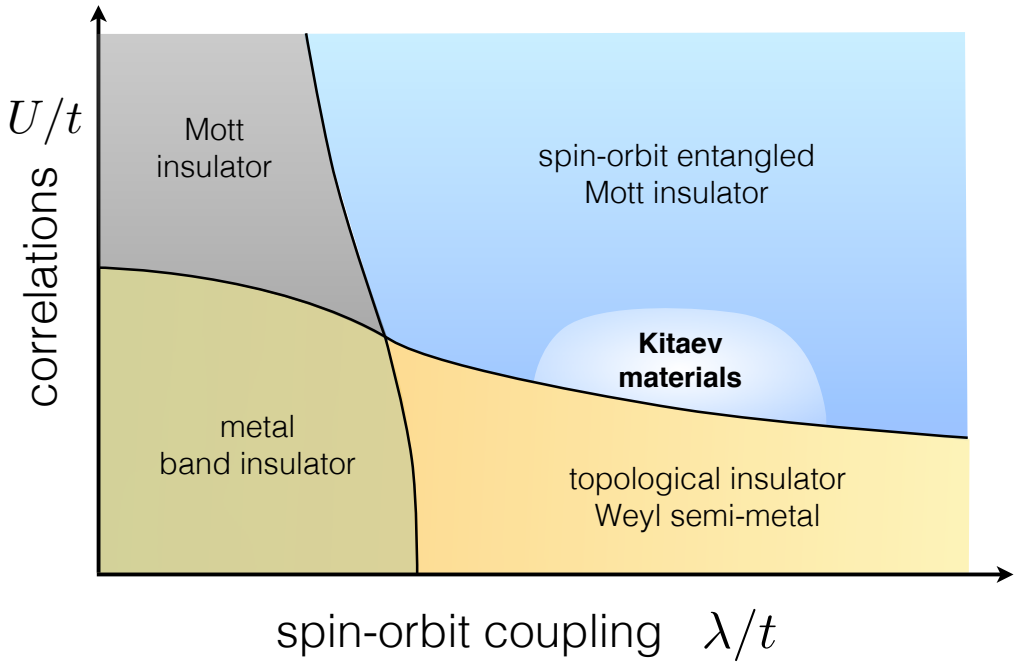

Fig. 6: Spin-orbit assisted Mott insulators. *Shown is a conceptual phase diagram in the presence of correlations (Hubbard U) and spin-orbit coupling λ. The four quadrants of this phase diagram exhibit distinct behavior. For small U and λ we are in the realm of non-interacting electronic band structures, which allow for the formation of metals and band insulators. Cranking up the spin-orbit coupling one can induce a band inversion to create a topological band insulator (or, similarly, a topological semi-metal). For strong correlations we expect to see Mott insulators, which in the presence of strong spin-orbit coupling can turn into a distinct class of Mott insulators with local, spin-orbit entangled moments. The Kitaev materials of interest in this chapter form a subclass of these spin-orbit entangled Mott insulators as discussed in the text. Figure adapted from Reference [3].*

This is where the new class of spin-orbit entangled Mott insulators enter the game. To conceptually understand what these new types of Mott insulators are, it is quite instructive to consider a general phase diagram in the presence of electronic correlations, i.e., a Hubbard U, and spin-orbit coupling λ as it is mapped out in Figure 6. Let us start in the lower left corner of this phase diagram, i.e., in the limit of small correlations and small spin-orbit coupling. This is the realm of non-interacting band theory which tells us that there are two principal states of matter – metals and band insulators. If one now adds substantial spin-orbit coupling, i.e., one moves to the right in the phase diagram, we have learned that, for a band insulator, this can lead to a band inversion and the formation of a topological band insulator [39,40] with protected gapless surface modes. Similarly, we can also create a topological metal via strong spin-orbit coupling, such as a Weyl semi-metal [41]. Now, let us add electronic correlations to the mix. In the regime of small spin-orbit coupling we know that electronic correlations can induce an insulating state of matter that is distinct from a band insulator – a so-called Mott insulator (which, in contrast to band insulators, can occur even at half filling). The local moments in such an electronic Mott insulator are typically $SU(2)$ spin-1/2 (or higher-spin) degrees of freedom – a good place to im-

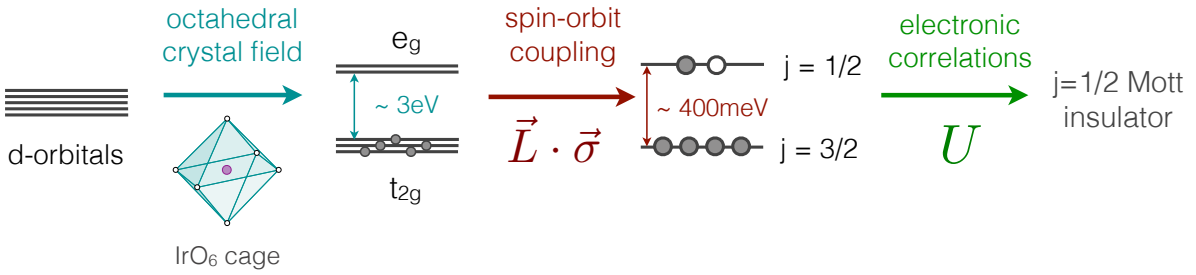

Fig. 7: Spin-orbit entanglement. *Schematic illustration of the formation of spin-orbit entangled $j{=}1/2$ moments in $5d^5$ or $4d^5$ materials with five electrons in the d orbital. Placing such d-orbitals within an octahedral crystal field such as an IrO_6 cage will split the five orbitals into three low-energy t_{2g} orbitals and two high-lying e_g orbitals. The five electrons with a total spin $s{=}1/2$ in the low-lying t_{2g} orbital with an effective orbital moment $l{=}1$ will experience further level splitting upon the introduction of strong spin-orbit coupling. This will result in a low-lying, completely filled $j{=}3/2$ and high-lying, half-filled $j{=}1/2$ state. This $j{=}1/2$ multiplet can now be turned into a Mott insulating states with an effective $j{=}1/2$ moment with relative small electronic correlations (Hubbard U).*

plement a Heisenberg model. If, however, we crank up the spin-orbit coupling in this strongly correlated regime we might end up in a different type of Mott insulator – so-called spin-orbit entangled Mott insulators, in which the local degrees of freedom have both spin and orbital components that are intimately linked to one another.

This scenario plays out in a class of $5d$ and $4d$ materials, which we will now zoom in on. Specifically, we will be interested in $5d^5$ and $4d^5$ materials, that is d-orbitals which are occupied with 5 electrons. This is, for instance, the case for the Iridates, in which the $5d$ iridium ions typically have an electronic Ir^{4+} configuration, and also for $RuCl_3$ with its $4d$ Ru^{3+} ions. As schematically illustrated in Figure 7, a conspiracy of crystal-field splitting, spin-orbit coupling and relatively weak electronic correlations can turn such materials into Mott insulators with local, spin-orbit entangled moments. Historically, this was somewhat unexpected to happen since one might expect $4d$ and particularly $5d$ materials to generically form metallic states, which – compared to the standard class of $3d$ Mott insulators such as the cuprates – exhibit much larger atoms resulting in relatively large electronic overlap in their crystalline structures, which would have to be compensated by strong electronic correlations. But the increased atomic size also gives rise to a much enhanced spin-orbit coupling, which in a crude estimation scales with the fourth power of the atomic number, $\lambda \propto Z^4$. It is through this spin-orbit coupling that the Mott lobes of the $j{=}1/2$ (and $j{=}3/2$) states exhibit a much smaller bandwidth and a relatively small amount of electronic correlations can split them to form Mott insulating states. As such these Mott insulators are also called "spin-orbit assisted" Mott insulators [3]. Their physical reality was first observed, some fifteen years ago, in 2008 in experiments on the perovskite iridate Sr_2IrO_4 [42, 43]. The latter is an isostructural analogue of La_2CuO_4, the parent compound of the cuprate superconductors, which, at the time, set off a flurry of activities searching for (topological) superconductivity in the presence of strong spin-orbit coupling [4].

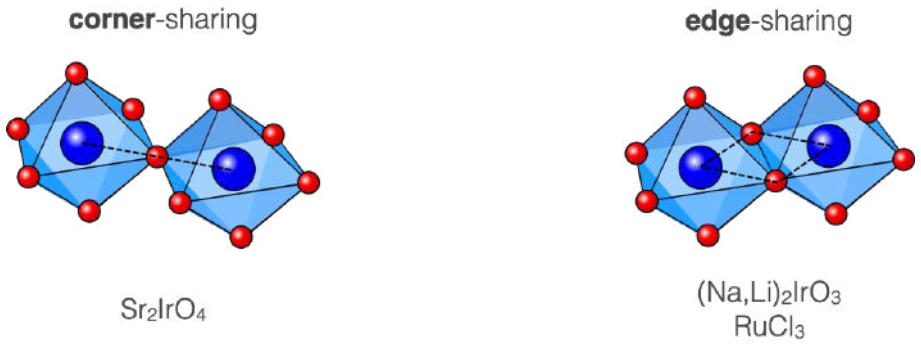

Fig. 8: Exchange path geometries. *The lattice geometries of perovskite and honeycomb iridates (and related materials) distinguish themselves by the way the elementary octahedral oxygen cages are connected – either in a corner-sharing fashion for the perovskite iridates such as $SrIr_2O_4$, while the honeycomb iridates such as Na_2IrO_3 exhibit edge-sharing geometries. The effect on the exchange of the $j{=}1/2$ moments (at the center of the octahedral cages) is profound: while the corner-sharing geometry gives rise to Heisenberg interactions, the edge-sharing geometry exhibits a dominant bond-directional Kitaev-type exchange.*

Prior to these experimental developments, Giniyat Khaliullin had already worked out a $j{=}1/2$ moments theory [44], which would consider the effect of different lattice geometries on the exchange paths of such spin-orbit entangled moments and their resulting effective interactions. In particular, two scenarios have turned out to make a crucial distinction as depicted schematically in Figure 8. Whereas the perovskite iridates exhibit a corner-sharing, square lattice geometry of the octahedral oxygen cages, other iridates with an underlying honeycomb lattice geometry would have edge-sharing oxygen cages. This difference in corner- versus edge-sharing geometries turns out to heavily influence the microscopic exchange of the spin-orbit entangled $j{=}1/2$ moments at the center of the octahedral cages. While in the corner-sharing scenario one finds an isotropic Heisenberg exchange, the edge-sharing scenario induces a suppression of this isotropic Heisenberg exchange (via destructive interference of two Ir-O-Ir exchange paths) turning the next-order bond-directional exchange into the dominant coupling. This turns out to be the sought-after Kitaev-type interaction which we have been looking for.

5 Kitaev materials

In 2009 Jackeli and Khaliullin turned this thinking about spin-orbit entangled $j{=}1/2$ Mott insulators with edge-sharing geometries into a concrete proposal – they went out and postulated that honeycomb iridates such as Na_2IrO_3 and Li_2IrO_3 should be an ideal place to look for Kitaev physics [45]. The boldness of this proposal should be appreciated – while we might have become accustomed to the idea that we can theoretically predict materials properties of weakly-coupled materials and then await experimental verification in a newly synthesized compound (this has been a recurring motif in the synthesis of topological insulators), such a conceptual prediction for strongly-correlated Mott materials has been without much precedent. Nevertheless, this proposal turned out to be extremely influential and opened the field of Kitaev spin liquid physics to experimental exploration of actual materials which rapidly happened.

5.1 Honeycomb iridates Na_2IrO_3 and Li_2IrO_3

The first samples of Na_2IrO_3 were synthesized basically within a year of the theoretical proposal by the groups of Takagi [46] and Gegenwart [47]. Many other groups would follow and today single crystals of Na_2IrO_3 are readily available in labs around the world. But there was an element of initial disillusion too – Na_2IrO_3 exhibits an ordering transition [48] around $T_N \approx 15$ K, i.e., it is clearly not showing a quantum disordered spin liquid ground state. Resonant X-ray magnetic scattering [49] and neutron scattering experiments [50, 51] would later reveal that the local moments form a zig-zag order. But on the positive side, the local moments themselves would turn out to be indeed the sought-after spin-orbit entangled $j{=}1/2$ moments, as seen from magnetic susceptibility measurements [47, 48]. Another uplift came when a direct experimental observation of bond-directional exchange was reported in diffuse magnetic X-ray scattering experiments [52], which later would be substantiated as Kitaev-type interactions in resonant inelastic X-ray spectroscopy (RIXS) [53]. It also posed new puzzles such as the observation of short-range spin-spin correlations in RIXS experiments [54, 27] on temperature scales far above the ordering temperature, see Figure 5. Such a high-temperature formation of spin-spin correlations would be a signature of a low-temperature Kitaev spin liquid as argued in the earlier section on thermal signatures of fractionalization. So maybe Na_2IrO_3 is, after all, not that far away from spin liquid physics?

Such puzzles coming out of the experimental exploration of the first Kitaev candidate material, Na_2IrO_3, have spurred more theoretical activity. Starting with the addition of a Heisenberg interaction to the pure Kitaev model [24, 25, 55–58], the effect of more and more perturbations of the Kitaev model have been explored leading to a refined microscopic model [59]

$$H = \sum_{\gamma-\text{bonds}} J\ \mathbf{S}_i\mathbf{S}_j + K\ S_i^\gamma S_j^\gamma + \Gamma\left(S_i^\alpha S_j^\beta + S_i^\beta S_j^\alpha\right),$$

which also includes a bond-directional, off-diagonal Γ-exchange. Complementing this more and more detailed microscopic understanding, the general concept of a "proximate spin liquid" [60, 61] was developed whose central idea is sketched in Figure 9. While additional "non-Kitaev" interactions (as in the Hamiltonian above) might induce magnetic ordering (as observed, for instance, in Na_2IrO_3), there might be a window of opportunity (indicated by the red arrow in the figure) to observe some of the thermal signatures of a nearby/proximate spin liquid ground state. Physically this finite-temperature proximate spin liquid regime opens up, as the free energy of a thermal spin liquid state (with all its fluctuations) is generically expected to be lower than the free energy of a thermally excited magnetically ordered state (which shows little fluctuations). It might be in this regime that we indeed see remnants of spin liquid physics above magnetically ordered states, such as signatures of fractionalization and the unexpected build-up of local spin-spin correlations [27].

The synthesis of the sister compound Li_2IrO_3 has led to yet another surprising discovery – this material exists in several polymorphs [48,62,63] which have been dubbed α-Li_2IrO_3, β-Li_2IrO_3, and γ-Li_2IrO_3 in the sequence of their discovery. The first one, α-Li_2IrO_3, is a honeycomb material akin to Na_2IrO_3, which shares most of its experimental signatures: local $j{=}1/2$ moments

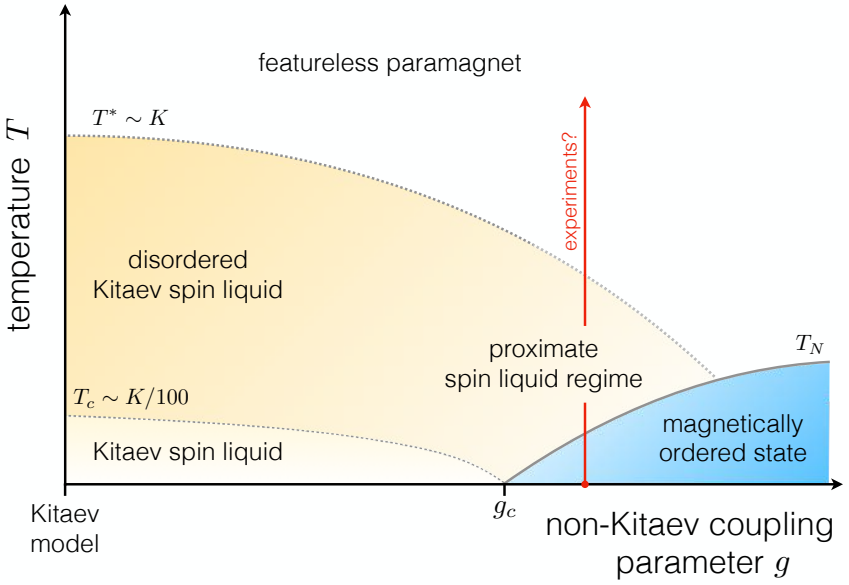

Fig. 9: Proximate spin liquid. *Conceptual phase diagram of the Kitaev model perturbed by some additional interactions parametrized by a coupling strength g, such as a Heisenberg and/or off-diagonal Γ-exchange, that will induce some type of magnetic ordering if sufficiently strong, $g > g_c$. At finite temperatures we would expect the spin liquid state, stabilized as a ground state for $g < g_c$, to dominate over the magnetically ordered state, since its fluctuations will lower its effective free energy more strongly than those of the ordered state. As such the magnetic ordering transition will bend to the right as indicated. This, however, opens a temperature window, indicated by the red arrow, in which one might see the thermal signatures of the proximate spin liquid such as the thermal fractionalization crossover and accompanying build-up of local spin-spin correlations shown in Figure 5.*

form, but undergo a magnetic ordering transition at $T_N \approx 15$ K to what is a somewhat unusual magnetic ordering pattern with counter-rotating spin spirals [64–66]. The other two polymorphs are materials in which the local $j{=}1/2$ moments are arranged in *three-dimensional* lattice geometries. These lattice structures, however, retain an important ingredient of the honeycomb lattice – they are still *tri-coordinated*, i.e., every site is connected to only three other sites (which is a highly unusual setting in a three-dimensional geometry), just as in the honeycomb case and the two polymorphs, β-Li_2IrO_3, and γ-Li_2IrO_3 have been dubbed hyperhoneycomb and stripy honeycomb to convey this point. Experimentally, these two 3D polymorphs turn out to be relatively close to their 2D counterpart in that they exhibit an ordering transition to a counter-rotating spin spiral state.

But again experimental discovery has spurred theoretical advances, here in the form of an investigation of three-dimensional generalizations of the Kitaev model [67,68]. The key observation is that the tri-coordination of the 3D lattice geometries still allows for the same analytical approach devised by Kitaev for the 2D honeycomb geometry (via a four Majorana fermion decomposition and subsequent bond-wise recombination, as illustrated in Figure 4). This has led to an extensive classification of three-dimensional Kitaev models, both in terms of their spin liquid ground states which can be recast as different types of Majorana metals [34] as well as their thermodynamic signatures [31].

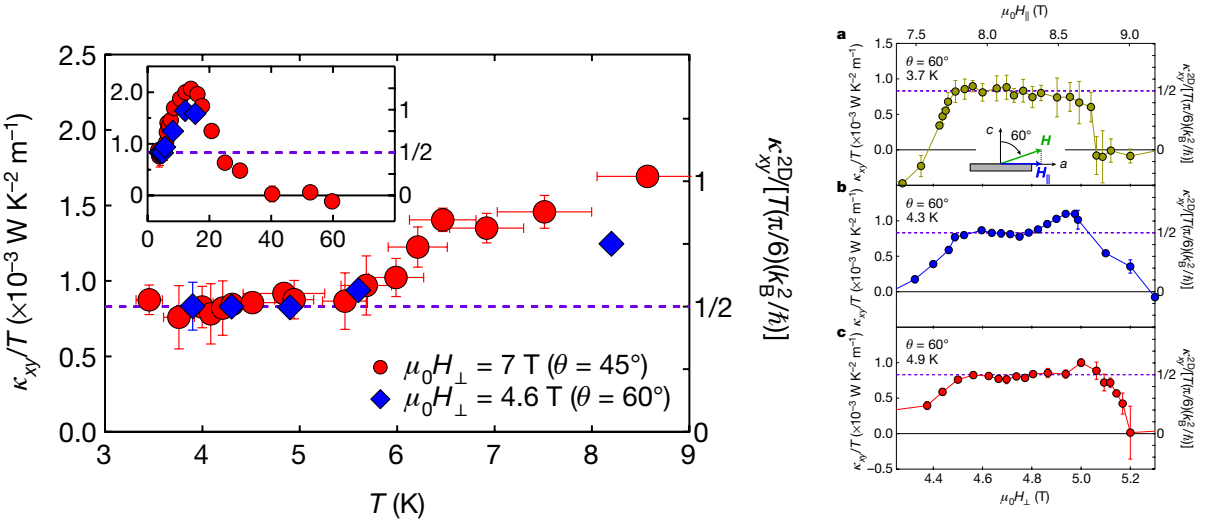

Fig. 10: Quantized Thermal Hall Effect. *Thermal Hall conductivity of α-RuCl$_3$ in a tilted magnetic field. (left) The thermal Hall conductivity κ_{xy}/T appears to saturate at a 1/2-quantized value within a temperature range of 4–6 K (for two tilted magnetic field configurations). The inset shows the higher-temperature behavior of κ_{xy}/T, overshooting the half-quantized value with increasing temperature and reaching a maximum at $\sim 14K$ before decreasing again for even higher temperatures. (right) The thermal Hall conductivity as a function of increasing magnetic field, at a fixed angle of 60° away from the c-axis for the three different temperatures. The plateau appears to be stable over an extended field and temperature range. Figure adapted from Ref. [75].*

5.2 α-RuCl$_3$

The biggest impact on the field of Kitaev materials has come in the form of the $4d$ compound α-RuCl$_3$, which had long existed but has been appreciated as another candidate material for honeycomb Kitaev physics only in 2014 [69]. By then a well-oiled sequence of initial experiments set in which quickly established the $j{=}1/2$ nature of the local moments [70, 71] and again the onset of zig-zag order [61], though at a slightly lower temperature of $T_N \approx 7$ K. But what sets α-RuCl$_3$ apart from the two honeycomb iridates discussed above has been a second round of spectacular experiments that have solidified its status as a front runner to indeed exhibit telltale signatures of Kitaev spin liquid physics. The first came in the interpretation of Raman scattering data as having *fermionic* excitations across a broad energy and temperature range [72–74], indicating the absence of a conventional magnetic state which only has bosonic excitations (magnons and phonons), but allowing for a more speculative state such as the Kitaev spin liquid which would indeed exhibit (Majorana) fermion excitations. The second in the form of the observation of a diffuse scattering continuum [60,61] in the inelastic neutron scattering of α-RuCl$_3$, reminiscent of what one would expect for fractional excitations such as spinons or, in the context of Kitaev models – spinless Majorana fermions. This observation at finite excitation energies above a magnetically ordered ground state is what triggered the conceptual idea of a proximate spin liquid, introduced in the previous section.

The most spectacular experimental result, reported by the Matsuda group in Kyoto [75], has come in the form of a field-induced state that appears to exhibit a half-quantized thermal Hall effect over a temperature range of 4–6 K, different orientations of the tilted magnetic field, and an extended plateau forming as a function of the magnetic field strength, as reproduced in Figure 10. It is precisely such a 1/2-quantized thermal Hall effect that one would theoretically expect for the field-induced, chiral spin liquid mentioned in the theory introduction. While gapped in the bulk, this chiral spin liquid would have gapless Majorana edge modes that would carry precisely a 1/2 (thermal) charge quantum. While similar to electronic fractional quantum Hall states (such as the one introduced [76] for filling fraction $\nu{=}5/2$, which gained experimental support through careful thermal Hall measurements [77]), an important difference is that the electronic Hall state arises due to the formation of Landau levels (and Coulomb interactions). In contrast, the chiral spin liquid state at hand is a non-trivial Chern insulator of Majorana fermions. One important distinction between the two scenarios is that the latter can also form in a *planar* field configuration, while the formation of Landau levels always requires an out-of-plane field component. As such, it has been quite reassuring to see that the Matsuda group could indeed reproduce their observation of a thermal Hall plateau for such an in-plane field configuration only [78]. There is grain of salt, however, in that these results have only been partially reproduced by the Takagi group [79], while others have openly questioned the quality of the quantization and have instead argued that the observation of quantum oscillations in fact points to the formation of a field-induced gapless spin liquid [80].

We are left to state that the observation of a field-induced Kitaev spin liquid remains a much-discussed topic in the community of Kitaev material aficionados that will come to a final conclusion only by further experimental evidence or all-encompassing theoretical models. Or to put it with a more positive spin – there is still much to be done here.

5.3 Other materials

Following the initial proposal [45] of the honeycomb iridates Na_2IrO_3 and Li_2IrO_3, a plethora of alternative compositions of honeycomb iridates have been put forward and synthesized, including $H_3LiIr_2O_6$ [81], $Ag_3LiIr_2O_6$ [82] and $Cu_3LiIr_2O_6$ [83], in which the interlayer alkali Li ions of Li_2IrO_3 have been replaced by H, Ag or Cu, respectively. In a similar vain, but starting from Na_2IrO_3, we have seen the synthesis of $Cu_3NaIr_2O_6$ [83] and Cu_2IrO_3 [84]. For readers interested in learning more about this "second generation" of honeycomb Kitaev materials we point to our recent review of Kitaev materials [2].

Going beyond the Jackeli-Khaliullin mechanism, much recent attention has gone into the question whether $3d^7$ materials such as cobaltates can also exhibit Kitaev physics [85,86], despite the reservation one might have that these systems will exhibit considerably smaller spin-orbit coupling than the $4d$ and $5d$ compounds discussed so far. Initial experimental efforts have focused on $Na_2Co_2TeO_6$ [87, 88] and $Na_3Co_2SbO_6$ [87] as potentially interesting materials, which like their d^5 counterparts both exhibit zigzag magnetic order at low temperatures [89–91]. Inelastic neutron scattering measurements have been argued to show evidence for dominant Kitaev

exchange interactions [92, 93], though this interpretation still remains under debate. Application of a magnetic field to $Na_2Co_2TeO_6$ points to a field-induced disordered state that could potentially harbor spin liquid physics [94, 95]. For another set of cobaltates, $BaCo_2(AsO_4)_2$ and $BaCo_2(PO_4)_2$, which have also been considered to be potential Kitaev materials, it by now seems increasingly likely that their original theoretical description, in terms of an XXZ J_1-J_2-J_3 model, better captures their essential physics [96–99].

In further broadening the search for Kitaev materials, it may be worthwhile to look beyond $4d$ and $5d$ transition metals and consider rare-earth magnets [100] whose $4f$ electrons are much more localized than the $5d$ or $4d$ electrons in iridates and ruthenates and at the same time experience a considerably stronger spin-orbit coupling – thus potentially providing another path to Kitaev materials in the future. New materials that realize antiferromagnetic Kitaev interactions, in contrast to the ferromagnetic interactions believed to occur in the current set of known Kitaev materials, will be particularly welcome both as a means to explore a new area of the extended phase diagrams and for their distinct in-field properties. At the level of materials synthesis, the search for Kitaev materials continues unabated.

If we adopt an even broader definition of what a Kitaev material (or Kitaev magnet) is by requiring that a given material is (i) a spin-orbit entangled Mott insulators with local $j{=}1/2$ moments, which (ii) interact via bond-directional Kitaev-type interactions, a much broader class of materials comes into view. In particular, these might realize lattice geometries well beyond the honeycomb structure of the original Kitaev model. This includes, for instance, the double perovskite Ba_2CeIrO_6, which turns out to be a pristine $j{=}1/2$ Mott insulator where the moments are subject to frustrated magnetism on the face-centered cubic lattice with Kitaev interactions [101].

6 Outlook

The field of Kitaev materials has come a long way since its inception by the introduction of the Kitaev honeycomb model [14] in 2006 and the bold proposal in 2009 to look for its physics in transition-metal oxides [45]. Along the way, we have seen one compound after the other being synthesized in unprecedented speed – broadening the search well beyond the initial trio of Na_2IrO_3, Li_2IrO_3, and α-$RuCl_3$ to other iridates, ruthenates, and even cobaltates. Experimental exploration has kept the pace and showered us with results, some of which reporting highly unusual observations that point to quantum spin liquid physics, such as Raman scattering data pointing to fermionic excitations, inelastic neutron scattering data showing a broad diffusive spectrum indicating fractionalized excitations, and a half-integer quantized thermal Hall effect. Further experimental efforts will need to go in the validation and verification of these results on different samples and by complementary approaches. On the theory side, the experimental discoveries have spurred lots of activities in refining the microscopic description of Kitaev materials beyond the pure Kitaev model, devising new concepts such as proximate spin liquid physics, and classifying Kitaev physics also in three-dimensional lattice geometries.

Looking into the future is impossible in a field with so much activity. But one might wish for some developments that seem promising today. On a materials synthesis side, this will include ideas to engineer novel Kitaev materials in hybrid devices such as heterostructures of α-$RuCl_3$ and graphene [102–104]. On the experimental side, novel probes such as two-dimensional coherent spectroscopy (2DCS) [105] to pick up the non-linear response of, for instance, fractional excitations might turn out to be rather insightful. Such novel spectroscopic methods should, of course, be complemented by theoretical activities predicting such non-linear response for the various Kitaev magnets of interest [106].

References

[1] S. Trebst, arXiv:1701.07056

[2] S. Trebst and C. Hickey, Phys. Rep. **950**, 1 (2022)

[3] W. Witczak-Krempa, G. Chen, Y.B. Kim, and L. Balents, Annu. Rev. Condens. Matter Phys. **5**, 57 (2014)

[4] J.G. Rau, E.K.-H. Lee, and H.-Y. Kee, Annu. Rev. Condens. Matter Phys. **7**, 195 (2016)

[5] S.M. Winter, A.A. Tsirlin, M. Daghofer, J. van den Brink, Y. Singh, P. Gegenwart, and R. Valentí, J. Phys.: Condens. Matter **29**, 493002 (2017)

[6] Y. Motome and J. Nasu, J. Phys. Soc. Jpn **89**, 012002 (2020)

[7] G.H. Wannier, Phys. Rev. **79**, 357 (1950)

[8] G.H. Wannier, Phys. Rev. B **7**, 5017 (1973)

[9] C.L. Henley, Annu. Rev. Condens. Matter Phys. **1**, 179 (2010)

[10] M. Levin and X.-G. Wen, Phys. Rev. Lett. **96**, 110405 (2006)

[11] A. Kitaev and J. Preskill, Phys. Rev. Lett. **96**, 110404 (2006)

[12] V. Kalmeyer and R.B. Laughlin, Phys. Rev. Lett. **59**, 2095 (1987)

[13] L. Savary and L. Balents, Rep. Prog. Phys. **80**, 016502 (2017)

[14] A. Kitaev, Ann. Phys. **321**, 2 (2006)

[15] M. Hermanns, I. Kimchi, and J. Knolle, Annu. Rev. Condens. Matter Phys. **9**, 17 (2018)

[16] Z. Nussinov and J. van den Brink, Rev. Mod. Phys. **87**, 1 (2015)

[17] A.Y. Kitaev, Ann. Phys. **303**, 2 (2003)

[18] E.H. Lieb, Phys. Rev. Lett. **73**, 2158 (1994)

[19] F.J. Burnell and C. Nayak, Phys. Rev. B **84**, 125125 (2011)

[20] C. Hickey and S. Trebst, Nat. Commun. **10**, 530 (2019)

[21] N.D. Patel and N. Trivedi, PNAS **116**, 12199 (2019)

[22] M. Gohlke, R. Moessner, and F. Pollmann, Phys. Rev. B **98**, 014418 (2018)

[23] Z. Zhu, I. Kimchi, D.N. Sheng, and L. Fu, Phys. Rev. B **97**, 241110 (2018)

[24] J. Chaloupka, G. Jackeli, and G. Khaliullin, Phys. Rev. Lett. **105**, 027204 (2010)

[25] H.-C. Jiang, Z.-C. Gu, X.-L. Qi, and S. Trebst, Phys. Rev. B **83**, 245104 (2011)

[26] X.-Y. Song, Y.-Z. You, and L. Balents, Phys. Rev. Lett. **117**, 037209 (2016)

[27] A. Revelli, M. Moretti Sala, G. Monaco, C. Hickey, P. Becker, F. Freund, A. Jesche, P. Gegenwart, T. Eschmann, F.L. Buessen, S. Trebst, P.H.M. van Loosdrecht, J. van den Brink, and M. Grüninger, Phys. Rev. Research **2**, 043094 (2020)

[28] E.Y. Loh, J.E. Gubernatis, R.T. Scalettar, S.R. White, D.J. Scalapino, and R.L. Sugar, Phys. Rev. B **41**, 9301 (1990)

[29] A.W. Sandvik, Phys. Rev. B **59**, R14157 (1999)

[30] J. Nasu, M. Udagawa, and Y. Motome, Phys. Rev. Lett. **113**, 197205 (2014)

[31] T. Eschmann, P.A. Mishchenko, K. O'Brien, T.A. Bojesen, Y. Kato, M. Hermanns, Y. Motome, and S. Trebst, Phys. Rev. B **102**, 075125 (2020)

[32] N. Read and S. Sachdev, Phys. Rev. Lett. **66**, 1773 (1991)

[33] T. Senthil and M.P.A. Fisher, Phys. Rev. B **62**, 7850 (2000)

[34] K. O'Brien, M. Hermanns, and S. Trebst, Phys. Rev. B **93**, 085101 (2016)

[35] G. Baskaran, S. Mandal, and R. Shankar, Phys. Rev. Lett. **98**, 247201 (2007)

[36] J. Knolle, D.L. Kovrizhin, J.T. Chalker, and R. Moessner, Phys. Rev. Lett. **112**, 207203 (2014)

[37] J. Knolle, D.L. Kovrizhin, J.T. Chalker, and R. Moessner, Phys. Rev. B **92**, 115127 (2015)

[38] G.B. Halász, N.B. Perkins, and J. van den Brink, Phys. Rev. Lett. **117**, 127203 (2016)

[39] M.Z. Hasan and C.L. Kane, Rev. Mod. Phys. **82**, 3045 (2010)

[40] X.-L. Qi and S.-C. Zhang, Rev. Mod. Phys. **83**, 1057 (2011)

[41] B. Yan and C. Felser, Annu. Rev. Condens. Matter Phys. **8**, 11.1 (2017)

[42] B.J. Kim, H. Jin, S.J. Moon, J.-Y. Kim, B.-G. Park, C.S. Leem, J. Yu, T.W. Noh, C. Kim, S.-J. Oh, J.-H. Park, V. Durairaj, G. Cao, and E. Rotenberg, Phys. Rev. Lett. **101**, 076402 (2008)

[43] B.J. Kim, H. Ohsumi, T. Komesu, S. Sakai, T. Morita, H. Takagi, and T. Arima, Science **323**, 1329 (2009)

[44] G. Khaliullin, Prog. Theor. Phys. Suppl. **160**, 155 (2005)

[45] G. Jackeli and G. Khaliullin, Phys. Rev. Lett. **102**, 017205 (2009)

[46] H. Takagi, *private communication* (2009)

[47] Y. Singh and P. Gegenwart, Phys. Rev. B **82**, 064412 (2010)

[48] Y. Singh, S. Manni, J. Reuther, T. Berlijn, R. Thomale, W. Ku, S. Trebst, and P. Gegenwart, Phys. Rev. Lett. **108**, 127203 (2012)

[49] X. Liu, T. Berlijn, W.-G. Yin, W. Ku, A. Tsvelik, Y.-J. Kim, H. Gretarsson, Y. Singh, P. Gegenwart, and J.P. Hill, Phys. Rev. B **83**, 220403 (2011)

[50] F. Ye, S. Chi, H. Cao, B.C. Chakoumakos, J.A. Fernandez-Baca, R. Custelcean, T.F. Qi, O.B. Korneta, and G. Cao, Phys. Rev. B **85**, 180403 (2012)

[51] S.K. Choi, R. Coldea, A.N. Kolmogorov, T. Lancaster, I.I. Mazin, S.J. Blundell, P.G. Radaelli, Y. Singh, P. Gegenwart, K.R. Choi, S.-W. Cheong, P.J. Baker, C. Stock, and J. Taylor, Phys. Rev. Lett. **108**, 127204 (2012)

[52] S. Hwan Chun, J.-W. Kim, J. Kim, H. Zheng, C.C. Stoumpos, C.D. Malliakas, J.F. Mitchell, K. Mehlawat, Y. Singh, Y. Choi, T. Gog, A. Al-Zein, M.M. Sala, M. Krisch, J. Chaloupka, G. Jackeli, G. Khaliullin, and B.J. Kim, Nat. Phys. **11**, 462 (2015)

[53] M. Magnaterra, K. Hopfer, C.J. Sahle, M.M. Sala, G. Monaco, J. Attig, C. Hickey, I.M. Pietsch, F. Breitner, P. Gegenwart, M.H. Upton, J. Kim, S. Trebst, P.H.M. van Loosdrecht, J. van den Brink, and M. Grüninger, arXiv:2301.08340

[54] J. Kim, J. c. v. Chaloupka, Y. Singh, J.W. Kim, B.J. Kim, D. Casa, A. Said, X. Huang, and T. Gog, Phys. Rev. X **10**, 021034 (2020)

[55] I. Kimchi and Y.-Z. You, Phys. Rev. B **84**, 180407 (2011)

[56] R. Schaffer, S. Bhattacharjee, and Y.B. Kim, Phys. Rev. B **86**, 224417 (2012)

[57] E. Sela, H.-C. Jiang, M.H. Gerlach, and S. Trebst, Phys. Rev. B **90**, 035113 (2014)

[58] I. Rousochatzakis, J. Reuther, R. Thomale, S. Rachel, and N.B. Perkins, Phys. Rev. X **5**, 041035 (2015)

[59] J.G. Rau, E.K.-H. Lee, and H.-Y. Kee, Phys. Rev. Lett. **112**, 077204 (2014)

[60] A. Banerjee, C.A. Bridges, J.Q. Yan, A.A. Aczel, L. Li, M.B. Stone, G.E. Granroth, M.D. Lumsden, Y. Yiu, J. Knolle, S. Bhattacharjee, D.L. Kovrizhin, R. Moessner, D.A. Tennant, D.G. Mandrus, and S.E. Nagler, Nat. Mater. **15**, 733 (2016)

[61] A. Banerjee, J. Yan, J. Knolle, C.A. Bridges, M.B. Stone, M.D. Lumsden, D.G. Mandrus, D.A. Tennant, R. Moessner, and S.E. Nagler, Science **356**, 1055 (2017)

[62] T. Takayama, A. Kato, R. Dinnebier, J. Nuss, H. Kono, L.S.I. Veiga, G. Fabbris, D. Haskel, and H. Takagi, Phys. Rev. Lett. **114**, 077202 (2015)

[63] K.A. Modic, T.E. Smidt, I. Kimchi, N.P. Breznay, A. Biffin, S. Choi, R.D. Johnson, R. Coldea, P. Watkins-Curry, G.T. McCandless, J.Y. Chan, F. Gandara, Z. Islam, A. Vishwanath, A. Shekhter, R.D. McDonald, and J.G. Analytis, Nat. Commun. **5**, 4203 (2014)

[64] I. Kimchi, R. Coldea, and A. Vishwanath, Phys. Rev. B **91**, 245134 (2015)

[65] E.K.-H. Lee and Y.B. Kim, Phys. Rev. B **91**, 064407 (2015)

[66] E.K.-H. Lee, J.G. Rau, and Y.B. Kim, Phys. Rev. B **93**, 184420 (2016)

[67] M. Hermanns and S. Trebst, Phys. Rev. B **89**, 235102 (2014)

[68] M. Hermanns, K. O'Brien, and S. Trebst, Phys. Rev. Lett. **114**, 157202 (2015)

[69] K.W. Plumb, J.P. Clancy, L.J. Sandilands, V.V. Shankar, Y.F. Hu, K.S. Burch, H.-Y. Kee, and Y.-J. Kim, Phys. Rev. B **90**, 041112 (2014)

[70] Y. Kobayashi, T. Okada, K. Asai, M. Katada, H. Sano, and F. Ambe, Inorg. Chem. **31**, 4570 (1992)

[71] J.M. Fletcher, W.E. Gardner, A.C. Fox, and G. Topping, J. Chem. Soc. A, 1038 (1967)

[72] L.J. Sandilands, Y. Tian, K.W. Plumb, Y.-J. Kim, and K.S. Burch, Phys. Rev. Lett. **114**, 147201 (2015)

[73] L.J. Sandilands, Y. Tian, A.A. Reijnders, H.-S. Kim, K.W. Plumb, Y.-J. Kim, H.-Y. Kee, and K.S. Burch, Phys. Rev. B **93**, 075144 (2016)

[74] Y. Wang, G.B. Osterhoudt, Y. Tian, P. Lampen-Kelley, A. Banerjee, T. Goldstein, J. Yan, J. Knolle, H. Ji, R.J. Cava, J. Nasu, Y. Motome, S.E. Nagler, D. Mandrus, and K.S. Burch, npj Quantum Materials **5**, 14 (2020)

[75] Y. Kasahara, T. Ohnishi, Y. Mizukami, O. Tanaka, Sixiao Ma, K. Sugii, N. Kurita, H. Tanaka, J. Nasu, Y. Motome, T. Shibauchi, and Y. Matsuda, Nature **559**, 227 (2018)

[76] G. Moore and N. Read, Nucl. Phys. B **360**, 362 (1991)

[77] M. Banerjee, M. Heiblum, V. Umansky, D.E. Feldman, Y. Oreg, and A. Stern, Nature **559**, 205 (2018)

[78] T. Yokoi, S. Ma, Y. Kasahara, S. Kasahara, T. Shibauchi, N. Kurita, H. Tanaka, J. Nasu, Y. Motome, C. Hickey, S. Trebst, and Y. Matsuda, Science **373**, 568 (2021)

[79] J.A.N. Bruin, R.R. Claus, Y. Matsumoto, N. Kurita, H. Tanaka, and H. Takagi, Nat. Phys. **18**, 401 (2022)

[80] P. Czajka, T. Gao, M. Hirschberger, P. Lampen-Kelley, A. Banerjee, J. Yan, D.G. Mandrus, S.E. Nagler, and N.P. Ong, Nat. Phys. **17**, 915 (2021)

[81] K. Kitagawa, T. Takayama, Y. Matsumoto, A. Kato, R. Takano, Y. Kishimoto, S. Bette, R. Dinnebier, G. Jackeli, and H. Takagi, Nature **554**, 341 (2018)

[82] V. Todorova, A. Leineweber, L. Kienle, V. Duppel, and M. Jansen, J. Solid State Chem. **184**, 1112 (2011)

[83] J.H. Roudebush, K.A. Ross, and R.J. Cava, Dalton Trans. **45**, 8783 (2016)

[84] M. Abramchuk, C. Ozsoy-Keskinbora, J.W. Krizan, K.R. Metz, D.C. Bell, and F. Tafti, J. Am. Chem. Soc. **139**, 15371 (2017)

[85] H. Liu and G. Khaliullin, Phys. Rev. B **97**, 014407 (2018)

[86] R. Sano, Y. Kato, and Y. Motome, Phys. Rev. B **97**, 014408 (2018)

[87] L. Viciu, Q. Huang, E. Morosan, H. Zandbergen, N. Greenbaum, T. McQueen, and R. Cava, J. Solid State Chem. **180**, 1060 (2007)

[88] R. Berthelot, W. Schmidt, A. Sleight, and M. Subramanian, J. Solid State Chem. **196**, 225 (2012)

[89] E. Lefrançois, M. Songvilay, J. Robert, G. Nataf, E. Jordan, L. Chaix, C.V. Colin, P. Lejay, A. Hadj-Azzem, R. Ballou, and V. Simonet, Phys. Rev. B **94**, 214416 (2016)

[90] A.K. Bera, S.M. Yusuf, A. Kumar, and C. Ritter, Phys. Rev. B **95**, 094424 (2017)

[91] C. Wong, M. Avdeev, and C.D. Ling, J. Solid State Chem. **243**, 18 (2016)

[92] M. Songvilay, J. Robert, S. Petit, J.A. Rodriguez-Rivera, W.D. Ratcliff, F. Damay, V. Balédent, M. Jiménez-Ruiz, P. Lejay, E. Pachoud, A. Hadj-Azzem, V. Simonet, and C. Stock, Phys. Rev. B **102**, 224429 (2020)

[93] C. Kim, J. Jeong, G. Lin, P. Park, T. Masuda, S. Asai, S. Itoh, H.-S. Kim, H. Zhou, J. Ma, and J.-G. Park, arXiv:2012.06167

[94] G. Lin, J. Jeong, C. Kim, Y. Wang, Q. Huang, T. Masuda, S. Asai, S. Itoh, G. Günther, M. Russina, Z. Lu, J. Sheng, L. Wang, J. Wang, G. Wang, Q. Ren, C. Xi, W. Tong, L. Ling, Z. Liu, L. Wu, J. Mei, Z. Qu, H. Zhou, X. Wang, J.-G. Park, Y. Wan, and J. Ma, Nat. Commun. **12**, 5559 (2021)

[95] X. Hong, M. Gillig, R. Hentrich, W. Yao, V. Kocsis, A.R. Witte, T. Schreiner, D. Baumann, N. Perez, A.U.B. Wolter, Y. Li, B. Buchner, and C. Hess, Phys. Rev. B **104**, 144426 (2021)

[96] T. Halloran, F. Desrochers, E.Z. Zhang, T. Chen, L.E. Chern, Z. Xu, B. Winn, M.K. Graves-Brook, M.B. Stone, A.I. Kolesnikov, Y. Qui, R. Zhong, R. Cava, Y.B. Kim, and C. Broholm, arXiv:2205.15262 (2022)

[97] X. Liu and H.-Y. Kee, arXiv:2211.03737 (2022)

[98] S. Das, S. Voleti, T. Saha-Dasgupta, and A. Paramekanti, Phys. Rev. B **104**, 134425 (2021)

[99] P.A. Maksimov, A.V. Ushakov, Z.V. Pchelkina, Y. Li, S.M. Winter, and S.V. Streltsov, Phys. Rev. B **106**, 165131 (2022)

[100] F.-Y. Li, Y.-D. Li, Y. Yu, A. Paramekanti, and G. Chen, Phys. Rev. B **95**, 085132 (2017)

[101] A. Revelli, C.C. Loo, D. Kiese, P. Becker, T. Fröhlich, T. Lorenz, M. Moretti Sala, G. Monaco, F.L. Buessen, J. Attig, M. Hermanns, S.V. Streltsov, D.I. Khomskii, J. van den Brink, M. Braden, P.H.M. van Loosdrecht, S. Trebst, A. Paramekanti, and M. Grüninger, Phys. Rev. B **100**, 085139 (2019)

[102] B. Zhou, J. Balgley, P. Lampen-Kelley, J.-Q. Yan, D.G. Mandrus, and E.A. Henriksen, Phys. Rev. B **100**, 165426 (2019)

[103] S. Mashhadi, Y. Kim, J. Kim, D. Weber, T. Taniguchi, K. Watanabe, N. Park, B. Lotsch, J.H. Smet, M. Burghard, and K. Kern, Nano Lett. **19**, 4659 (2019)

[104] D.J. Rizzo, B.S. Jessen, Z. Sun, F.L. Ruta, J. Zhang, J.-Q. Yan, L. Xian, A.S. McLeod, M.E. Berkowitz, K. Watanabe, T. Taniguchi, S.E. Nagler, D.G. Mandrus, A. Rubio, M.M. Fogler, A.J. Millis, J.C. Hone, C.R. Dean, and D.N. Basov, Nano Lett. **20**, 8438 (2020)

[105] Y. Wan and N.P. Armitage, Phys. Rev. Lett. **122**, 257401 (2019)

[106] W. Choi, K.H. Lee, and Y.B. Kim, Phys. Rev. Lett. **124**, 117205 (2020)